Superconductivity and unexpected chemistry of germanium hydrides under pressure

M. Mahdi Davari Esfahani,[1] Artem R. Oganov,[2,1,3,4,*] Haiyang Niu,[1] and Jin Zhang[1]

[1]*Department of Geosciences, Center for Materials by Design, and Institute for Advanced Computational Science, State University of New York, Stony Brook, New York 11794-2100, USA*

[2]*Skolkovo Institute of Science and Technology, Skolkovo Innovation Center, 3 Nobel Street, Moscow 143026, Russia*

[3]*Department of Problems of Physics and Energetics, Moscow Institute of Physics and Technology, 9 Institutskiy Lane, Dolgoprudny City, Moscow Region 141700, Russia*

[4]*International Center for Materials Design, Northwestern Polytechnical University, Xi'an 710072, China*

(Received 30 October 2016; published 10 April 2017)

Following the idea that hydrogen-rich compounds might be high-T_c superconductors at high pressures, and the very recent breakthrough in predicting and synthesizing hydrogen sulfide with record-high $T_c = 203$ K, an *ab initio* evolutionary algorithm for crystal structure prediction was employed to find stable germanium hydrides. In addition to the earlier structure of germane with space group *Ama2*, we propose a *C2/m* structure, which is energetically more favorable at pressures above 278 GPa (with inclusion of zero-point energy). Our calculations indicate that the *C2/m* phase of germane is a superconductor with $T_c = 67$ K at 280 GPa. Germane is found to become thermodynamically unstable to decomposition to hydrogen and the compound Ge_3H_{11} at pressures above 300 GPa. Ge_3H_{11} with space group $I\bar{4}m2$ is found to become stable at above 285 GPa with $T_c = 43$ K. We find that the pressure-induced phase stability of germanium hydrides is distinct from analogous isoelectronic systems, e.g., Si hydrides and Sn hydrides. Superconductivity stems from large electron-phonon coupling associated with the wagging, bending, and stretching intermediate-frequency modes derived mainly from hydrogen.

DOI: 10.1103/PhysRevB.95.134506

High-throughput materials discovery using first-principles density functional theory (DFT) [1] has motivated many experimental studies. For years, scientists have been trying to find the best way to design high-temperature superconductors. It has been confirmed that high-T_c superconductivity can be found in systems with light elements. Hydrogen is the lightest element with rich structures and properties under high pressures. Within BCS (Bardeen-Cooper-Schrieffer) theory of superconductivity [2], high vibrational frequencies of hydrogen atoms and often high electron-phonon coupling (EPC) make it possible to expect high T_c in metallic hydrogen and hydrogen-rich hydrides.

However, metallic hydrogen seems to require very high pressure $\sim$ 400 GPa and proved elusive. Therefore, chemical precompression by alloying with heavy element was proposed [3]. Many theoretical and experimental studies have been motivated by this idea to seek and design new high-T_c superconductors at high pressures [4–15].

In a recent breakthrough discovery, which was first predicted by the evolutionary algorithm USPEX coupled with DFT [16], high-temperature superconductivity with a transition temperature (T_c) of 203 K in hydrogen sulfide H_3S under pressure 200 GPa has been reported by Drozdov *et al.* [15]. This discovery not only set a record high T_c for a conventional phonon-mediated mechanism but also raised hopes of reaching room-temperature superconductivity in hydrogen-rich metallic alloys. This realization is the best argument to show the predictive power of DFT-based structure prediction and electron-phonon coupling calculations, and opens up avenues for discovering superconductors based on this approach.

Successful synthesis of hydrogen sulfides with superconducting properties was followed by a second high-T_c hydrogen-rich compound at high pressure (PH_3) synthesized by Drozdov *et al.* [14]. Prior to H_3S, the highest experimentally observed T_c in conventional superconductors which obey the BCS theory was in MgB_2. However, other magnesium borides Mg_xB_y were shown to exhibit poor superconductivity with $T_c < 3$ K [11]. Besides these efforts, other superconductors have been predicted in hydrogen-rich compounds. In group-IV hydrides, SiH_4 has been predicted to have $T_c = 20$–75 K [17], while experiment got a lower value of 17 K [13]. Disilane (SiH_8) has been predicted to favor *Ccca* structure with T_c of 98–107 K at 250 GPa [18]. Our work on tin hydrides showed rich chemistry of that system with high-T_c superconductivity. Tin hydrides have been predicted to form at high pressures, exhibiting high T_c of 81, 93, and 97 K for SnH_8, SnH_{12}, and SnH_{14} at 220, 250, and 300 GPa, respectively [19]. In addition, novel linear and bent formations of H_3 and H_4 have been predicted to form in high-pressure phases of SnH_8, SnH_{12}, and SnH_{14} [19].

Germanium (Ge) is in the same group IV and is isovalent to Sn. One can expect germanium to exhibit similar chemistry as tin, but its smaller atomic radius and slightly higher electronegativity than Sn result in quite a different chemistry.

Germane (GeH_4) phases have been explored by Gao *et al.* [4] and their results show $C2/c - GeH_4$ becomes stable at pressures above 196 GPa [including zero-point energy (ZPE)] against decomposition into H and Ge. However, stability against decomposition into the elements is not a particularly stringent test, and stability against separation into other phases, e.g., GeH_4 into Ge_2H and H_2, which is important for understanding the decomposition mechanism, should be taken into account. *C2/c* was predicted to be a superconductor with $T_c = 64$ K at 220 GPa. In a recent theoretical study, a more energetically stable structure of germane (with symmetry

*artem.oganov@stonybrook.edu

group *Ama2*) was predicted by Zhang *et al.* to have T_c of 47–57 K [20]. Now, with major progress of computational methods (enabling, for example, variable-composition searches), we can address all the outstanding issues.

We systematically explored the high-pressure phase diagram of the Ge-H system using an evolutionary variable-composition search implemented in the USPEX code [21–24] from ambient pressure to 400 GPa. The effectiveness of this method has been shown by the prediction of high-pressure structures of various systems that were subsequently confirmed experimentally (e.g., [25–27]). In this method, we created the initial generation of structures and compositions using the random symmetric algorithm [28]. Subsequent generations were obtained using heredity, transmutation, softmutation, and random symmetric generator [28]. Ge hydrides, in comparison with other hydrides of the same group, e.g., Si [17,18] and Sn [19], which often show simpler phase diagrams, exhibit a unique and complex potential-energy landscape. Stoichiometries Ge_3H, Ge_2H, GeH_3, GeH_4, and Ge_3H_{11} emerge as stable at megabar pressures.

The underlying structure relaxations were carried out using the VASP package [29] in the framework of DFT and using PBE-GGA (Perdew-Burke-Ernzerhof generalized gradient approximation) [30]. The projector-augmented wave approach (PAW) [31] was used to describe the core electrons and their effects on valence orbitals. A plane-wave kinetic-energy cutoff of 1000 eV for hard PAW potentials and dense Monkhorst-Pack k-points grids with reciprocal space resolution $2\pi \times 0.03$ Å^{-1} were employed [32] to sample the Brillouin zone.

Phonon frequencies and superconducting properties were calculated using density-functional perturbation theory as implemented in the QUANTUM ESPRESSO package [33]. The PBE-GGA functional is used for this part. A plane-wave basis set with a cutoff of 80 Ry gave a convergence in energy with a precision of 1 meV/atom. We used valence electron configurations of $3d^{10}$,$4s^2$,$4p^2$, and $1s^1$ for germanium and hydrogen, respectively. Thermodynamic properties of germanium hydrides were calculated using the PHONOPY package with the implemented frozen-phonon approach [34].

The EPC parameter λ was calculated using $5 \times 5 \times 2$ and $4 \times 4 \times 4$ q-point meshes for $I\bar{4}m2 - Ge_3H_{11}$ and $C2/m - GeH_4$, respectively. Denser k-point meshes $20 \times 20 \times 8$ and $16 \times 16 \times 16$ were used in the calculations of the electron-phonon interaction matrix elements. The superconducting T_c was estimated using the Allen-Dynes modified McMillan equation [35].

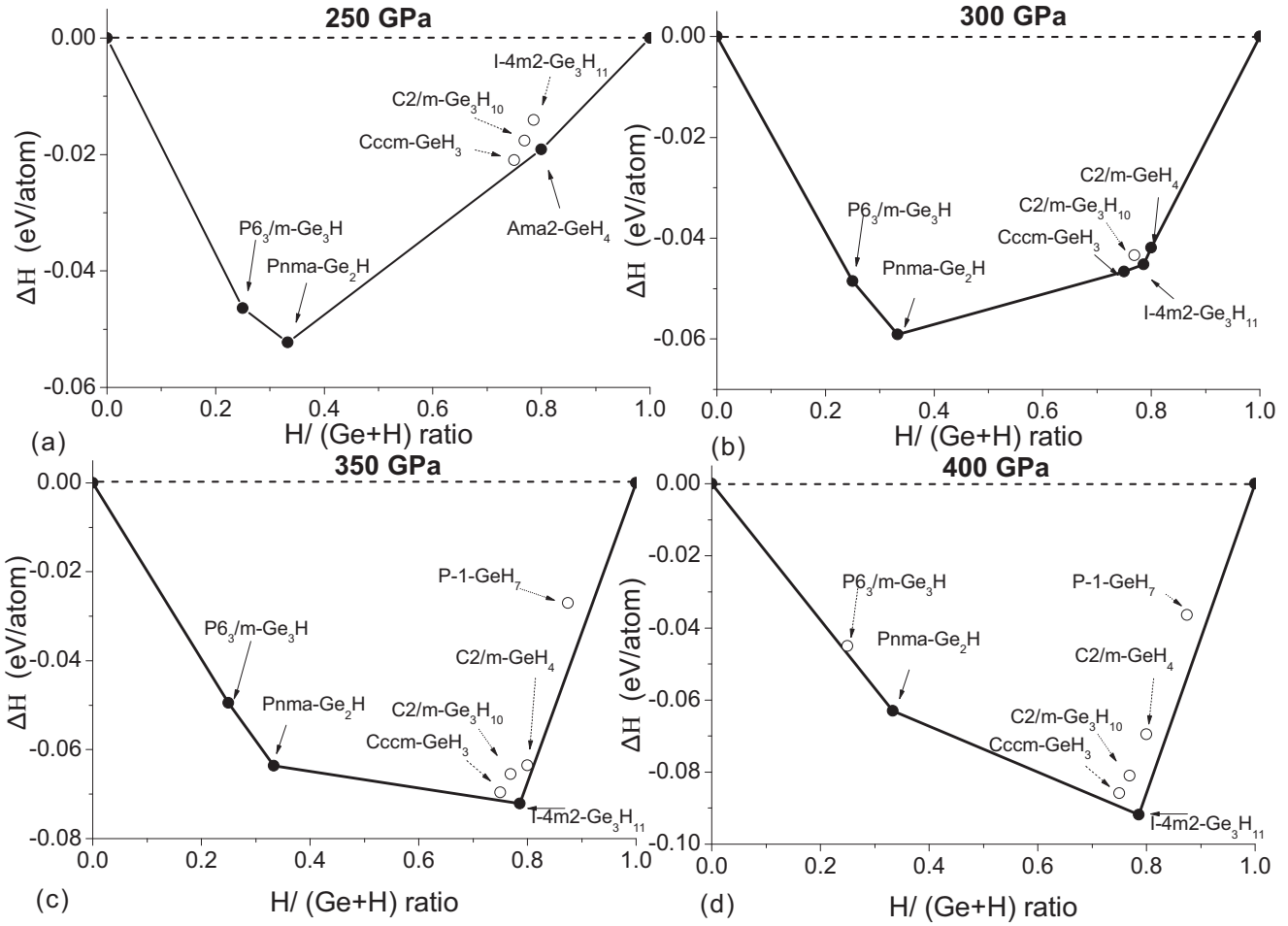

FIG. 1. Predicted formation enthalpy of $Ge_{1-x}H_x$ as a function of H concentration at selected pressures. Open circles above the convex hull show unstable compounds with respect to decomposition into the two adjacent phases on the convex hull, while solid circles show thermodynamically stable compounds. Pure Ge structures are consistent with [37], and pure H phases are taken from [38].

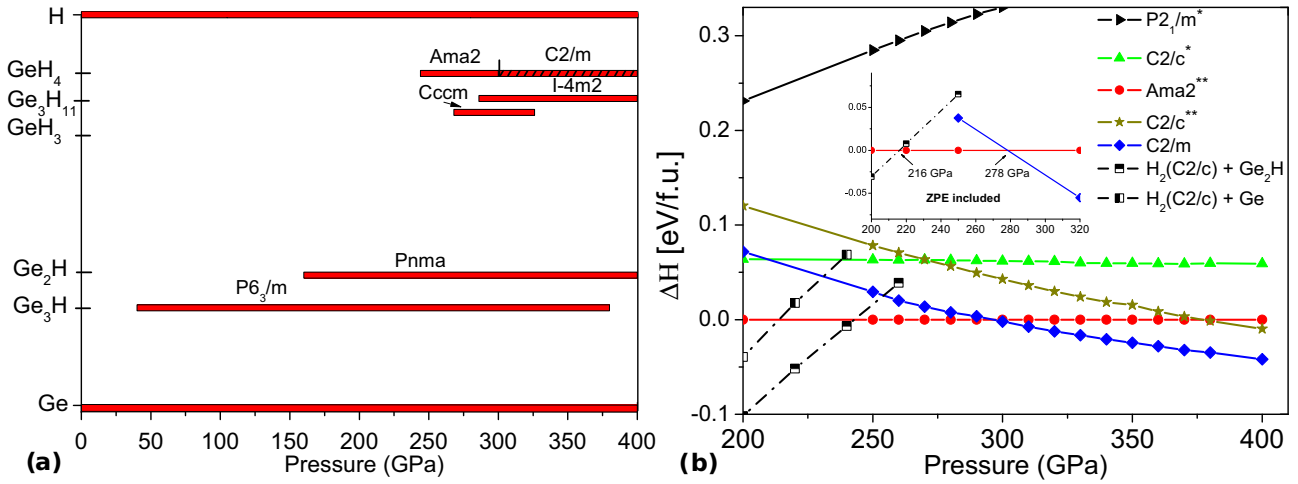

FIG. 2. (a) Predicted pressure-composition phase diagram of the Ge-H system. The dashed areas represent thermodynamically metastable structures. (b) The enthalpies per formula unit of various structures of germane as a function of pressure with respect to the previously reported *Ama2* structure [20]. Decomposition (GeH_4) enthalpies are calculated by adopting the *C2/c* structure for H_2 ([38]) and Ge_2H in the *Pnma* structure. The elemental decomposition enthalpies are also added for comparison. Inset: Enthalpies for *C2/m* structure relative to *Ama2* structure with zero-point corrections. The superscripts "*" and "**" represent the structures predicted by Gao *et al.* [4] and Zhang *et al.* [20], respectively.

The energetic stability of a variety of Ge_xH_y $(x + y < 20)$ compounds was evaluated using the thermodynamic convex hull construction at different pressures, as depicted in Fig. 1. To our surprise, in addition to reproducing various structures of the Ge-H system [4,9,20,36], Ge [37] and H_2 [38], previously unreported and unexpected composition Ge_3H_{11} was found to be stable in wide pressure range.

Below 200 GPa, no hydrogen-rich composition is stable against decomposition into the elements. This is consistent with not having any solid H-rich Ge hydrides at low pressures, although using *in situ* gas-condensation techniques Maley *et al.* showed germane can form at ambient pressure [39]. Increasing pressure decreases formation enthalpies, implying a tendency for Ge hydrides to be stabilized under further compression. Phases of elemental hydrogen for the convex hull construction were obtained from structure search, in good agreement with the ones reported in [38]. For elemental Ge, we obtained a complex phase diagram with at least four phase transitions between 70 and 400 GPa, which are in good agreement with [37].

At 250 GPa, the tetragonal Ge_3H_{11} with space group $I\bar{4}m2$ is still metastable and lies just above the tie-line joining $Ama2 - GeH_4$ and $Pnma - Ge_2H$. At 300 GPa, we predict stable phases: Ge_3H $(P6_3/m)$,Ge_2H $(Pnma)$, and GeH_3 $(Cccm)$ in accord with previous predictions [9,20]. In addition, we also found unexpected composition Ge_3H_{11} that appears in the H-rich region, its structure featuring GeH_{12} distorted icosahedra and GeH_{16} Frank-Casper polyhedra. Moreover, germane transforms to a new monoclinic phase with space group *C2/m* with 3 f.u./cell at above 300 GPa (278 GPa with inclusion of ZPE), which is lower in enthalpy than all previously proposed structures [4,9,20] [see also Fig. 2(b)].

The stability fields of solids Ge_3H, Ge_2H, GeH_3, Ge_3H_{11}, and GeH_4 are illustrated in a pressure-composition phase diagram of the Ge-H system, as shown in Fig. 2(a). Ge-rich compounds tend to stabilize at lower pressure (<200 GPa), while higher pressure (>200 GPa) is required for H-rich compounds to form. To the best of our knowledge, these unexpected yet complex stoichiometries have not been reported in group-IV hydrides except MH_4 (M = Si, Sn, Pb). This rich

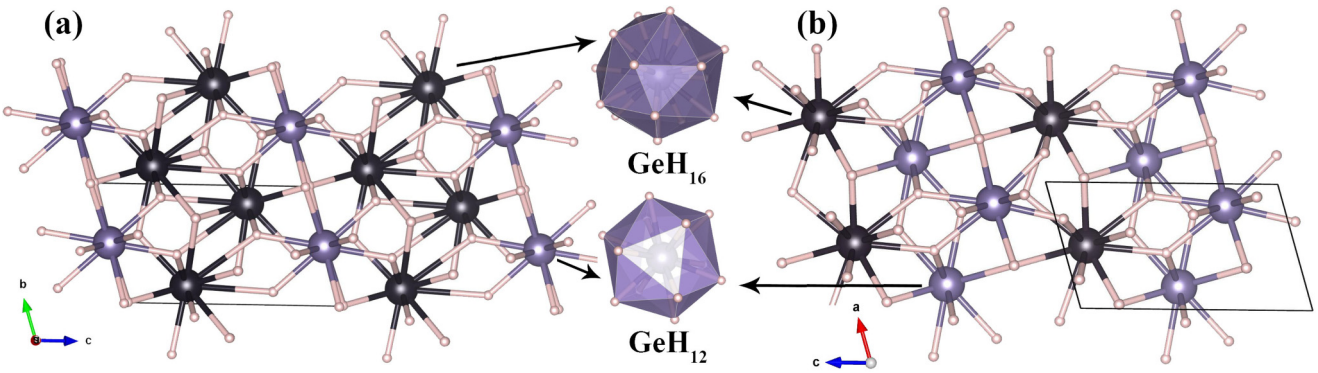

FIG. 3. Predicted structures of Ge-H compounds at high pressures: (a) GeH_4 in the *C2/m* structure and (b) Ge_3H_{11} in the $I\bar{4}m2$ structure. Small and large spheres represent H and Ge atoms, respectively. Different colors of germanium atoms represent different types of polyhedra, i.e., black spheres represent GeH_{16} polyhedra and purple spheres show GeH_{12} icosahedra.

TABLE I. Predicted crystal structures of Ge_3H_{11} and GeH_4 at 300 GPa.

Phase	Lattice parameters	Atom	x	y	z
$I\bar{4}m2-Ge_3H_{11}$	$a=2.891$ Å	Ge_1(4e)	0.0000	0.0000	0.1750
	$c=9.845$ Å	Ge_2(2b)	0.0000	0.0000	0.5000
		H_1(8i)	0.2248	0.0000	0.3320
		H_2(8i)	0.7377	0.0000	0.0351
		H_3(4f)	0.0000	0.5000	0.1031
		H_4(2c)	0.0000	0.5000	0.2500
$C2/m-GeH_4$	$a=10.226$ Å	Ge_1(2b)	0.0000	0.5000	0.0000
	$b=2.967$ Å	Ge_2(4i)	0.8483	0.0000	0.6037
	$c=2.922$ Å	H_1(8j)	0.3501	0.2383	0.1187
	$\beta=74.46^\circ$	H_2(4i)	0.2822	0.0000	0.9765
		H_3(4i)	0.2806	0.0000	0.6187
		H_4(4i)	0.4274	0.0000	0.5731
		H_5(4i)	0.9953	0.0000	0.7488

chemistry makes Ge hydrides of special interest. It can be seen that the formation of Ge_3H_{11} at 285 GPa lowers the convex hull and finally around 300 GPa causes GeH_4 to become thermodynamically metastable. The dynamical stabilities of structures shown in Fig. 2(a) were confirmed in their pressure ranges of stability via phonon calculations.

GeH_4 was predicted to become stable against decomposition into the elements at above 225 GPa (196 GPa with the inclusion of zero-point energy) [4], while our results reveal lower enthalpy of Ge_2H+H_2 indicating the need for somewhat higher pressure 244 GPa (216 GPa with ZPE inclusion) for GeH_4 to be stabilized [see Fig. 2(b) inset]. Upon increasing pressure, the *Ama2* structure of GeH_4 transforms into the *C2/m* structure at 300 GPa. Structures predicted in the literature are also included for comparison. In the *Ama2* $\rightarrow$ *C2/m* transition, the coordination number of Ge atoms increases from 10 to 12 and 16 with the formation of GeH_{12} distorted icosahedra and GeH_{16} Frank-Casper polyhedra at 300 GPa [Fig. 3(a) inset]. In addition, the average Ge-H bond lengths slightly increase from 1.698 to 1.704 Å in the *Ama2* $\rightarrow$ *C2/m* transition.

GeH_4 is unstable against decomposition to H_2 (*Cmca*) and Ge_3H_{11} ($I\bar{4}m2$) at pressures above 300 GPa, according to the convex hull [see Figs. 1(b) and 1(c)]. Similarly, GeH_3 decomposes to Ge_2H and Ge_3H_{11}.

Both in $I\bar{4}m2-Ge_3H_{11}$ and $C2/m-GeH_4$, each Ge atom is coordinated with 12 and 16 H atoms making distorted icosahedra and GeH_{16} Frank-Casper polyhedra (see Fig. 3). The average Ge-H bond lengths are 1.660 and 1.704 Å in $I\bar{4}m2-Ge_3H_{11}$ and $C2/m-GeH_4$ at 300 GPa, respectively. Unlike other compressed hydrides [5,19,40,41], there are no bonds between H atoms.

As shown in Fig. 3, liberating one hydrogen atom from a 3-f.u. cell turns a GeH_{16} polyhedra into a less coordinated germanium atom and leads to the formation of a distorted icosahedron, i.e., GeH_4 consists of two GeH_{16} polyhedra and a GeH_{12} icosahedron, however Ge_3H_{11} turns out to have one GeH_{16} polyhedron and two distorted icosahedra. The detailed crystallographic data are listed in Table I.

Because of high concentration of hydrogen in GeH_4, contribution of ZPE would be important in determining the relative stability of hydrogen-rich phases [4,6,19,42,43]. However, our results show that ZPE does not change the topology of the phase diagram of GeH_4, and quantitative effects are just moderate shifts in transition pressures. For example, the inclusion of ZPE lowers the formation enthalpies of *Ama2* and *C2/m* structures and shifts the transition pressure *Ama2* $\rightarrow$ *C2/m* from 300 to 278 GPa, indicating enhanced stability of the *C2/m* phase owing to ZPE [see Fig. 2(b) inset].

Analyzing the electronic band structures of GeH_4 (*C2/m*) and Ge_3H_{11} ($I\bar{4}m2$) [see Figs. 4(a) and 4(b)] indicates indirect band overlap which results in metallic behavior, with highly dispersive bands crossing the Fermi level, these bands being basically due to germanium states with p character and marginally due to hydrogen states with s character. These H-derived states near Fermi level resemble those of solid metallic hydrogen. The *C2/m* structure is a metal with several electron and hole pockets at the Fermi level. In the energy region near E_f, the DOS of Ge is about two times that of

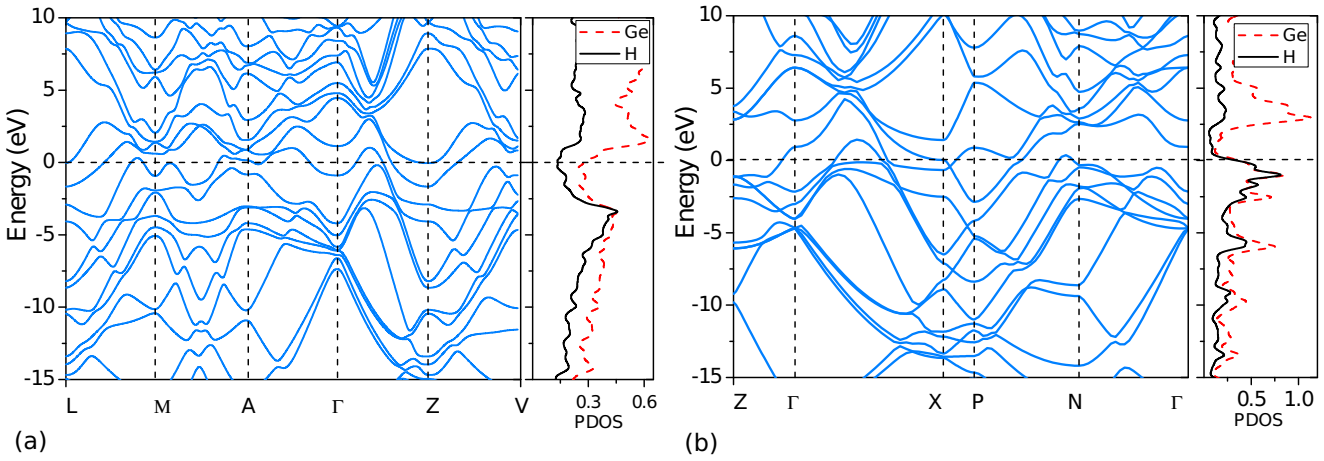

FIG. 4. Electronic band structure along with the projected electronic DOS of (a) GeH_4 in the *C2/m* structure at 300 GPa and (b) Ge_3H_{11} in the $I\bar{4}m2$ structure at 300 GPa.

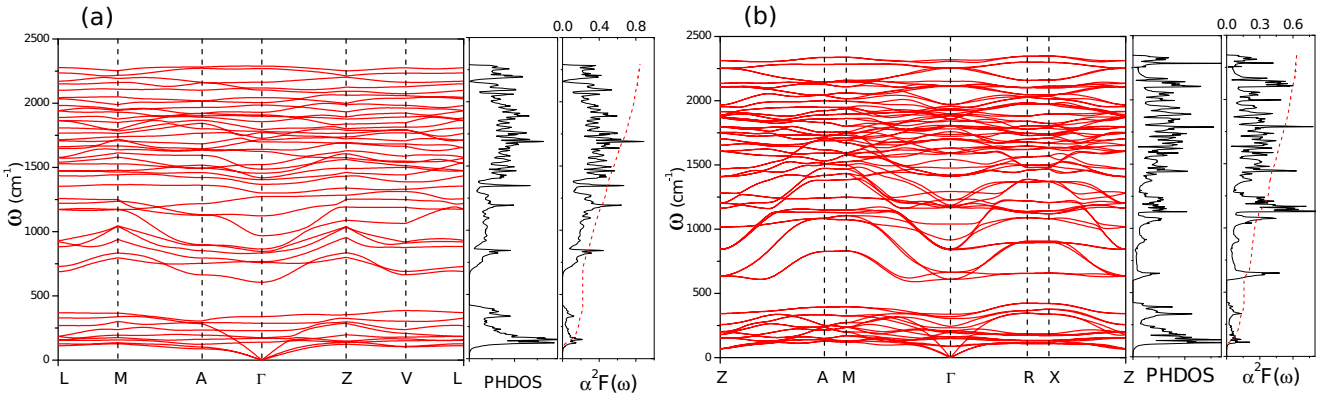

FIG. 5. Calculated phonon dispersion curves, phonon density of states (PHDOS), Eliashberg EPC spectral functions $\alpha^2F(\omega)$, and electron-phonon integral $\lambda(\omega)$ of (a) GeH_4 [*C2/m*] at 300 GPa and (b) Ge_3H_{11} [$I\bar{4}m2$] at 300 GPa.

H, which indicates the dominance of Ge atoms contribution to the bands near the Fermi level. The total DOS at E_f, $N(E_f)$, is 0.27 states/eV/f.u. for the $C2/m-GeH_4$ structure at 300 GPa, while we see higher $N(E_f) = 0.31$ for the *Ama2* phase at 300 GPa. The Fermi levels of GeH_4 and Ge_3H_{11} fall on a shoulder of the density of states, while the record T_c in H_3S is explained to be due to the van Hove singularity close to the Fermi level [44,45], therefore doping can be expected to raise $N(E_f)$ and T_c values. These values of DOS at the Fermi level $N(E_f)$ are lower than those in H_3S (0.54 states/eV/f.u.).

To probe the possible superconducting behavior, EPC calculations were performed for $C2/m-GeH_4$ and $I\bar{4}m2-Ge_3H_{11}$ structures at 280, 300, and 320 GPa. Phonon dispersions, phonon density of states, the corresponding Eliashberg spectral function $\alpha^2F(\omega)$, and the EPC parameter λ as a function of frequency are calculated and shown in Figs. 5(a) and 5(b) for $C2/m-GeH_4$ and $I\bar{4}m2-Ge_3H_{11}$ at 300 GPa, respectively.

The low-frequency bands below 430 cm^{-1} are mainly from the strongly coupled vibrations between Ge and H that contribute about 26% (25%) of the total λ, while higher-frequency phonons, predominantly wagging, bending, and stretching modes between 550 and 2300 cm^{-1} are mostly related to the H atoms bonded to Ge and contribute 74% (75%) of λ of the $C2/m-GeH_4$ ($I\bar{4}m2-Ge_3H_{11}$) phase.

The resulting integral λ and logarithmic average phonon frequencies (ω_{log}) are calculated using the Eliashberg formalism and then T_c values are estimated using the Allen-Dynes modified McMillan equation using Coulomb pseudopotential parameters $\mu^* = 0.1$ and 0.13 as commonly accepted values. Table II summarizes data for the total EPC parameters λ, logarithmic phonon average frequencies, and corresponding T_c values at given pressures.

Hard phonons in H-rich materials are expected to play an important role in high-T_c superconductivity [46], but because such hard phonons do not always produce large coupling constants, high-T_c superconductivity is still elusive. In the $C2/m-GeH_4$ structure, high-frequency vibrations that contribute the most to the EPC parameter produce a larger coupling constant, i.e., 25% higher than similar frequency modes in $I\bar{4}m2-Ge_3H_{11}$. Additional flat bands in the high-frequency region of $C2/m-GeH_4$ phonon modes can be ascribed to the higher coupling constant and eventually result in getting higher T_c value for $C2/m-GeH_4$.

We investigated the pressure dependence of the critical transition temperature. The results show that the calculated T_c decreases monotonically with pressure with approximate rates of −0.19 and −0.20 K/GPa for $C2/m-GeH_4$ and $I\bar{4}m2-Ge_3H_{11}$ in the pressure range 280–320 GPa. Higher T_c of the *C2/m* phase, compared to the previously reported phase $Ama2-GeH_4$, can be related to the considerably higher average phonon frequency.

In summary, we explored the high-pressure phase diagram of the Ge-H binary system by exploring its compositional and configurational space with an evolutionary crystal structure prediction method. Based on analysis of current and prior theoretical studies on Ge hydrides, we have established thermodynamically stable phases, superconducting properties, structural features, and decomposition lines in the pressure range 0–400 GPa.

At 250 GPa, all the stoichiometries Ge_2H, Ge_3H, and GeH_4 are energetically stable against any decomposition into the elements or any other compounds. At 300 GPa, GeH_3 and Ge_3H_{11} become stable, while GeH_4 becomes unstable.

TABLE II. The calculated EPC parameter (λ), logarithmic average phonon frequency (ω_{log}), and critical temperature (T_c) (with $\mu^* = 0.10$ and 0.13) for $C2/m-GeH_4$ and $I\bar{4}m2-Ge_3H_{11}$ at given pressures.

Structure	Pressure (GPa)	λ	ω_{log} (K)	T_c (K)
$C2/m-GeH_4$	280	0.895	1162	67 ($\mu^* = 0.10$)
				56 ($\mu^* = 0.13$)
	300	0.867	1154	63 ($\mu^* = 0.10$)
				52 ($\mu^* = 0.13$)
$I\bar{4}m2-Ge_3H_{11}$	285	0.721	1155	43 ($\mu^* = 0.10$)
				34 ($\mu^* = 0.13$)
	300	0.690	1140	38 ($\mu^* = 0.10$)
				29 ($\mu^* = 0.13$)
	320	0.668	1127	35 ($\mu^* = 0.10$)
				26 ($\mu^* = 0.13$)

A unique metallic phase of germane with *C2/m* space group is found to be energetically more favorable than all previously proposed structures at pressures above 278 GPa (if zero-point energy is included). Our results reveal that germane decomposes to hydrogen and the compound Ge_3H_{11} at the pressures above 300 GPa. According to electron-phonon coupling calculations, $C2/m-GeH_4$ and $I\bar{4}m2-Ge_3H_{11}$ are excellent superconductors with high T_c of 67 and 43 K for $C2/m-GeH_4$ at 280 GPa and $I\bar{4}m2-Ge_3H_{11}$ at 285 GPa, respectively.

ACKNOWLEDGMENTS

We thank the Defense Advanced Research Project Agency (Grant No. W31P4Q1210008) and the Russian Science Foundation (Grant No. 16-13-10459) for financial support. Calculations were performed on NSF Extreme Science and Engineering Discovery Environment facilities and on the cluster of the Center for Functional Nanomaterials, Brookhaven National Laboratory.

[1] W. Kohn and L. J. Sham, Phys. Rev. **140**, A1133 (1965).
[2] J. Bardeen, L. N. Cooper, and J. R. Schrieffer, Phys. Rev. **108**, 1175 (1957).
[3] N. W. Ashcroft, Phys. Rev. Lett. **92**, 187002 (2004).
[4] G. Gao, A. R. Oganov, A. Bergara, M. Martinez-Canales, T. Cui, T. Iitaka, Y. Ma, and G. Zou, Phys. Rev. Lett. **101**, 107002 (2008).
[5] X. Zhong, H. Wang, J. Zhang, H. Liu, S. Zhang, H.-F. Song, G. Yang, L. Zhang, and Y. Ma, Phys. Rev. Lett. **116**, 057002 (2016).
[6] I. Errea, M. Calandra, C. J. Pickard, J. R. Nelson, R. J. Needs, Y. Li, H. Liu, Y. Zhang, Y. Ma, and F. Mauri, Nature **532**, 81 (2016).
[7] G. Zhong, C. Zhang, X. Chen, Y. Li, R. Zhang, and H. Lin, J. Phys. Chem. C **116**, 5225 (2012).
[8] X.-F. Zhou, A. R. Oganov, X. Dong, L. Zhang, Y. Tian, and H.-T. Wang, Phys. Rev. B **84**, 054543 (2011).
[9] P. Hou, F. Tian, D. Li, Z. Zhao, D. Duan, H. Zhang, X. Sha, B. Liu, and T. Cui, RSC Adv. **5**, 19432 (2015).
[10] D. Duan, X. Huang, F. Tian, D. Li, H. Yu, Y. Liu, Y. Ma, B. Liu, and T. Cui, Phys. Rev. B **91**, 180502 (2015).
[11] M. M. Davari Esfahani, Q. Zhu, H. Dong, A. R. Oganov, S. Wang, M. S. Rakitin, and X.-F. Zhou, arXiv:1702.02221.
[12] V. V. Struzhkin, Physica C **514**, 77 (2015).
[13] M. I. Eremets, I. A. Trojan, S. A. Medvedev, J. S. Tse, and Y. Yao, Science **319**, 1506 (2008).
[14] A. Drozdov, M. Eremets, and I. Troyan, arXiv:1508.06224.
[15] A. Drozdov, M. Eremets, I. Troyan, V. Ksenofontov, and S. Shylin, Nature (London) **525**, 73 (2015).
[16] D. Duan, Y. Liu, F. Tian, D. Li, X. Huang, Z. Zhao, H. Yu, B. Q Liu, W. Tian, and T. Cui, Sci. Rep. **4**, 06968 (2014).
[17] X.-J. Chen, J.-L. Wang, V. V. Struzhkin, H.-k. Mao, R. J. Hemley, and H.-Q. Lin, Phys. Rev. Lett. **101**, 077002 (2008).
[18] T. A. Strobel, M. Somayazulu, and R. J. Hemley, Phys. Rev. Lett. **103**, 065701 (2009).
[19] M. M. D. Esfahani, Z. Wang, A. R. Oganov, H. Dong, Q. Zhu, S. Wang, M. S. Rakitin, and X.-F. Zhou, Sci. Rep. **6**, 22873 (2016).
[20] H. Zhang, X. Jin, Y. Lv, Q. Zhuang, Q. Lv, Y. Liu, K. Bao, D. Li, B. Liu, and T. Cui, Phys. Chem. Chem. Phys. **17**, 27630 (2015).
[21] A. R. Oganov, A. O. Lyakhov, and M. Valle, Acc. Chem. Res. **44**, 227 (2011).
[22] A. R. Oganov, Y. Ma, A. O. Lyakhov, M. Valle, and C. Gatti, Rev. Mineral. Geochem. **71**, 271 (2010).
[23] C. W. Glass, A. R. Oganov, and N. Hansen, Comput. Phys. Commun. **175**, 713 (2006).
[24] A. O. Lyakhov, A. R. Oganov, and M. Valle, Comput. Phys. Commun. **181**, 1623 (2010).
[25] W. Zhang, A. R. Oganov, A. F. Goncharov, Q. Zhu, S. E. Boulfelfel, A. O. Lyakhov, E. Stavrou, M. Somayazulu, V. B. Prakapenka, and Z. Konpkov, Science **342**, 1502 (2013).
[26] A. R. Oganov, J. Chen, C. Gatti, Y. Ma, Y. Ma, C. W. Glass, Z. Liu, T. Yu, O. O. Kurakevych, and V. L. Solozhenko, Nature (London) **457**, 863 (2009).
[27] A. J. Mannix, X.-F. Zhou, B. Kiraly, J. D. Wood, D. Alducin, B. D. Myers, X. Liu, B. L. Fisher, U. Santiago, J. R. Guest *et al.*, Science **350**, 1513 (2015).
[28] A. O. Lyakhov, A. R. Oganov, H. T. Stokes, and Q. Zhu, Comput. Phys. Commun. **184**, 1172 (2013).
[29] G. Kresse and J. Furthmüller, Phys. Rev. B **54**, 11169 (1996).
[30] J. P. Perdew, K. Burke, and M. Ernzerhof, Phys. Rev. Lett. **77**, 3865 (1996).
[31] P. E. Blöchl, Phys. Rev. B **50**, 17953 (1994).
[32] H. J. Monkhorst and J. D. Pack, Phys. Rev. B **13**, 5188 (1976).
[33] P. Giannozzi, S. Baroni, N. Bonini, M. Calandra, R. Car, C. Cavazzoni, D. Ceresoli, G. L. Chiarotti, M. Cococcioni, I. Dabo, A. Dal Corso, S. de Gironcoli, S. Fabris, G. Fratesi, R. Gebauer, U. Gerstmann, C. Gougoussis, A. Kokalj, M. Lazzeri, L. Martin-Samos, N. Marzari, F. Mauri, R. Mazzarello, S. Paolini, A. Pasquarello, L. Paulatto, C. Sbraccia, S. Scandolo, G. Sclauzero, A. P. Seitsonen, A. Smogunov, P. Umari, and R. M. Wentzcovitch, J. Phys.: Condens. Matter **21**, 395502 (2009).
[34] A. Togo and I. Tanaka, Scr. Mater. **108**, 1 (2015).
[35] P. B. Allen and R. C. Dynes, Phys. Rev. B **12**, 905 (1975).
[36] C. Zhang, X.-J. Chen, Y.-L. Li, V. V. Struzhkin, H.-K. Mao, R.-Q. Zhang, and H.-Q. Lin, Europhys. Lett. **90**, 66006 (2010).
[37] F. J. Ribeiro and M. L. Cohen, Phys. Rev. B **62**, 11388 (2000).
[38] C. J. Pickard and R. J. Needs, Nat. Phys. **3**, 473 (2007).
[39] I. J. Maley, D. H. Brown, R. M. Ibberson, and C. R. Pulham, Acta Crystallogr. B **64**, 312 (2008).
[40] D. Duan, F. Tian, X. Huang, D. Li, H. Yu, Y. Liu, Y. Ma, B. Liu, and T. Cui, arXiv:1504.01196.
[41] J. Hooper, B. Altintas, A. Shamp, and E. Zurek, J. Phys. Chem. C **117**, 2982 (2013).
[42] A. Shamp, T. Terpstra, T. Bi, Z. Falls, P. Avery, and E. Zurek, J. Am. Chem. Soc. **138**, 1884 (2016).
[43] H. Wang, S. T. John, K. Tanaka, T. Iitaka, and Y. Ma, Proc. Natl. Acad. Sci. USA **109**, 6463 (2012).
[44] Y. Quan and W. E. Pickett, Phys. Rev. B **93**, 104526 (2016).
[45] L. Ortenzi, E. Cappelluti, and L. Pietronero, Phys. Rev. B **94**, 064507 (2016).
[46] N. W. Ashcroft, Phys. Rev. Lett. **21**, 1748 (1968).